Yerbilimleri, 29 (1), 1-15
Hacettepe Üniversitesi Yerbilimleri Uygulama ve Araştırma Merkezi Dergisi
Journal of the Earth Sciences Application and Research Centre of Hacettepe University

Investigation of the seismic damage caused to the Gunung Sitoli (Tögi-Ndrawa) cave by the 2005 Great Nias earthquake

2005 Büyük Nias depreminin Gunung Sitoli (Tögi-Ndrawa) mağarasında neden olduğu sarsıntı hasarının incelenmesi

Ömer AYDAN
Tokai University, Department of Marine Civil Engineering,
Orido 3-20-1, Shizuoka, 424-8610, JAPAN

Geliş (*received*) : 14 Aralık (*December*) 2007
Kabul (*accepted*) : 03 Mart (*March*) 2008

ABSTRACT

The quantification of the seismic past of regions during a non-instrumental period is important for seismic design and disaster mitigation. The utilization of damage to the speleothems of caves as one of the tools of paleo-seismology has recently been receiving particular attention. The author investigated the Nias Island cave in relation to the 2005 Great Nias earthquake that accurred in Indonesia in July 2007. In the first part of this article, a brief outline of the seismo-tectonic and strong motion characteristics of the 2005 earthquake is given. Then the traces of the damage to speleothems by the 2005 Great Nias earthquake, as well as earlier large events, found in the cave of Gunung Sitoli in Nias Island during the investigation are presented and their implications are discussed. (There is no doubt that the utilization of damage to speleothems of caves is an important tool for the quantification of the seismic past.) Furthermore, the cave is also regarded as an underground rock structure and its stability is evaluated using available empirical and analytical methods. In addition, the susceptibility of seismic damage to stalactites and stalagmites is analytically evaluated using the seismic coefficient technique proposed and the implications are discussed.

Keywords: Nias Earthquake, seismic damage, stalactite, Tögi Ndrawa Cave.

ÖZ

Aletsel dönem öncesi bölgelerin depremselliğinin niceliksel olarak değerlendirilmesi oldukça önemlidir. Son yıllarda karstik mağaralardaki sarkıt ve dikitlerde oluşan hasarlar, aletsel dönem öncesi depremselliğin değerlendirilmesinde kullanılmaktadır. 2005 yılında meydana gelen Büyük Nias depreminde hasar gören Nias Adası karstik mağaradaki 2007 yılının Temmuz ayında incelenmiştir. Bu makalede önce 2005 Nias Adası'nda depreminin sismo-tektonik ve kuvvetli yer hareket özellikleri kısaca sunulmuştur. Daha sonra Nias adasında Gunung Sitoli veya Tögi Ndrawa olarak adlandırılan karstik mağaradaki sarkıt ve dikitlerde meydana gelmiş hasarlar sunulmuş ve 2005 Nias adası depremi ile daha önceki depremler arasındaki ilişkiler tartışılmıştır. Bu çalışmadan elde edilen en önemli sonuçlardan biri, hiç kuşkusuz, karstik mağaralardaki hasarların geçmişteki depremlerin belirlenmesinde oldukça kullanılabilir olmasıdır. Bunun yanı sıra, yeraltı kaya yapısı olarak, karstik

Ö. Aydan
E-posta: aydan@scc.u-tokai.ac.jp

mağaranın duraylılığı görgül ve analitik yöntemlerle değerlendirilmiştir. Sarkıt ve dikitlerin deprem sırasındaki hasar görme olasılığını incelemek üzere sismik katsayı yaklaşımına dayanan bir yöntem önerilmiş ve yapılan değerlendirmeler tartışılmıştır.

Anahtar Kelimeler: Nias depremi, sarsıntı hasarı, sarkıt, Tögi Ndrawa mağarası.

INTRODUCTION

An earthquake with a magnitude of 8.7 occurred on March 28, 2005 near Nias Island. This earthquake caused extensive damage to buildings, transporation facilities such as roadways and bridges in Nias Island as well as many slope and embankment failures. Furthermore, it induced extensive ground liquefaction and lateral spreading in sandy ground along the coastal area.

Karstic caves develop only in limestones along fracture zones caused by faulting movements. The percolation of rain water causes dissolution of limestone in the vicinity of fracture zones, resulting in huge caves. Earthquakes may cause damage to stalactites and stalagmites in karstic caves (Figure 1). Ground shaking, permanent fault movements or both may induce the damage to stalactites and stalagmites. The possibility of damage to stalactites is much higher than that to stalagmites.

The induced ground shaking was estimated to be greater than 0.3g in Nias Island. Therefore, the possibility of damage to stalactites in karstic caves in Nias Island was expected to be quite high. The damage may be observed as the fall of stalactites from the roofs of the caves. The GPS network operated by CalTech had recorded 4 m displacements in Lahewa. Therefore, the permanent ground deformations could also have induced damage to the caves in Nias Island.

Geological considerations estimated the possibility of karstic caves to be high in the vicinity of Gunung Sitoli. Furthermore, karstic caves may also be found near Lahewa, TelukDalam and Sirombu in view of the geology of the island. The author found from an Internet exploration that a cave exists near Gunnung Stoli, called Tögi Ndrawa (in Nias language this means inside the cave). In this article this which will be called the Gunung Sitoli cave.

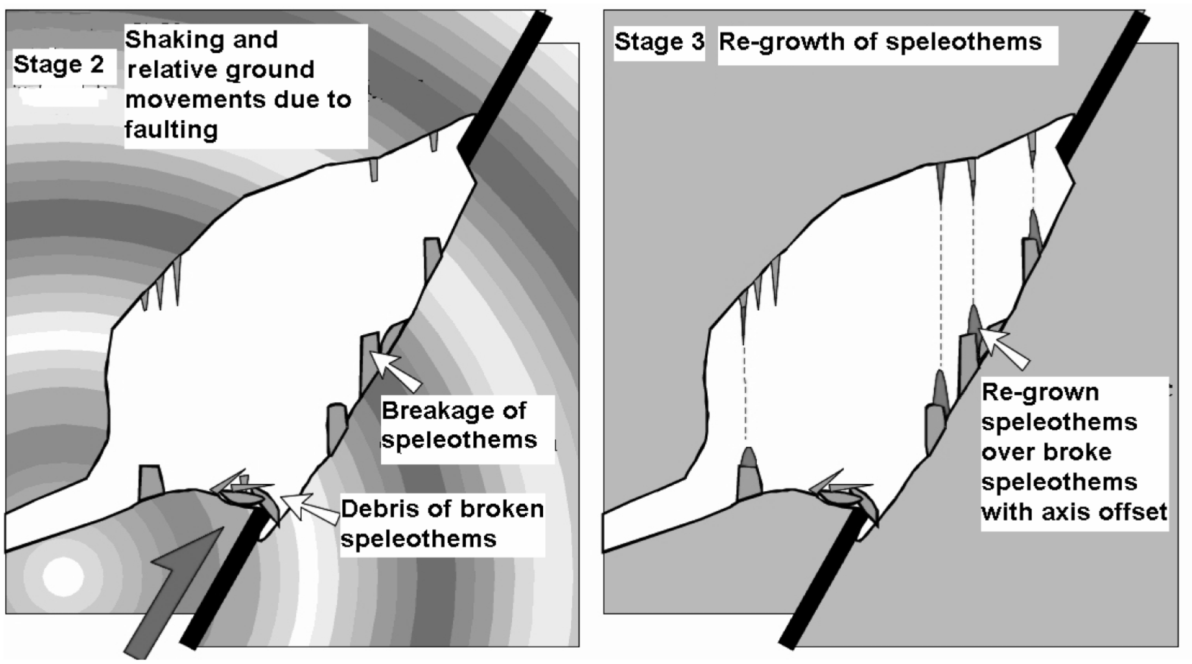

Figure 1. Illustration of damage to spleothem by earthquakes (modified from Gilli, 1999).
Şekil 1. Depremlerin sarkıt ve dikitlerde neden olduğu hasarların gösterimi (Gilli (1999)'dan değiştirilerek).

This paper is concerned with the damage in the Gunung Sitoli cave induced by the 2005 Great Nias earthquake and the observed damage and its characteristics are described. The investigation was carried out on July 31, 2007 about 28 months after the earthquake.

GEOGRAPHY AND GEOLOGY

Nias Island lies about 125 km west Sumatera Island in the Indian Ocean. It covers an area of 4771 km^2, which is mostly lowland area. The highest elevation is 886 m. It is the biggest in a group of islands on this side of Sumatra, which is a part of the province of Sumatera Utara. Nias is 140 km long and 50 km wide (Figure 2). The population in this area is about 639,675 people (including Malay, Batak, and Chinese. Gunung Sitoli is the capital city of Nias and it is the center of administration and business affairs of the regency.

The geological formations in Nias Island, according to Djamal et al. (1994), are named as alluvium, Gunung Sitoli formation, Gomo formation and Lelematua formation and melange (Figure 3). The alluvium belongs to Holocene and Quaternary, and it is encountered along shores and rivers.

The Gunung Sitoli formation consists mainly of limestone with intercalations of clay, weakly cemented sandstone and marl layers. Its geological age is Plio-Pleistocene and it is slightly folded. It has deposited in a shallow marine environment and unconformably overlies Gomo formation and Lelematua formation. Its thickness is about 120 m and karstic caves are found in this formation.

The Gomo and Lelematua formations include old volcanic rocks and consolidated sedimentary rocks. The thickness of the Gomo formation ranges between 1250 and 2500 m, while the thickness of the Lelematua formation is 3000 m in the eastern part and 2000 m in the middle of Nias Island. The Lelematua formation belongs to Miocene and unconformably overlies a melange complex. The melange complex stretches from northwest to southeast and was formed during Oligocene to early Miocene. It contains igneous and metamorphic rocks such as peridodite, serpentinite, basalt and schist.

Structural features such as faults, folds and lineaments generally trend northwest- southeast. Anticlines and synclines are generally asymmetric and some of them plunge northeast or southeast. Thrust faults are generally parallel to fold axes and dip northeast with an inclination of 30-40º and bound melange units with younger sedimentary deposits. Thrust faults and folds are crossed by strike-slip faults and normal faults. Lineaments found in Tertiary rocks trend northwest southeast. Tectonic activity and the related thrusting process of the melange units started in Oligocene. In Pliocene and Pleistocene, a tectonic phase caused faulting and uplifting of all units. This tectonic activity still continues today.

CHARACTERISTICS OF THE 2005 NIAS EARTHQUAKE AND STRONG MOTIONS

The USGS estimation of the magnitude (M_w) of the earthquake was 8.7 while HARVARD estimated that the moment magnitude (M_w) of the earthquake was 8.6 (Table 1). The epicenters determined by USGS (2005) and HARVARD (2005) differ from each other. While USGS (2005) estimated the hypocenter just beneath Banyak Island, HARVARD's epicenter was further SW and near Nias Island. Since the damage was much heavier in Nias Island, it seems that the estimation by HARVARD may be much closer to the actual epicenter. The faulting mechanism of the earthquake was also esti-

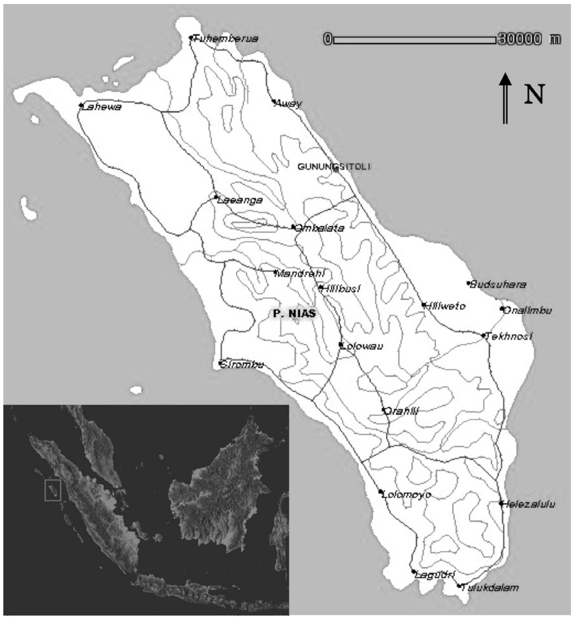

Figure 2. Location of Nias Island (OCHA, 2005).
Şekil 2. Nias adasının yeri (OCHA, 2005).

mated by the two institutes. The dominant faulting mechanism was inferred to be thrust-type by HARVARD, while USGS inferred the dominant faulting mechanism to be sinistral strike-slip. However, the fault plane is very gently inclined and its inclination ranges between 4°-7°. Yagi (2005) of BRI (presently Tsukuba University) inferred the slip propagation and estimated the relative slip at the hypocenter to be about 10 m (Table 2). Konca et al. (2006) recently re-analyzed seismic, geodetic and coral uplift observations (Figure 4). Their results are given together with those estimated by Yagi (2005) and Yamanaka (2005). These results indicate that the fault propagation proceeded beneath Nias Island. Konca et al. (2006) reported that the horizontal offset and vertical uplift at Lahewa GPS station were 4.5 m and 3 m, respectively.

The areas hit by tsunami were Singkil and Sibolga in Sumatra Island, Simeulue Island, Banyak Islands and Nias Island. The height of the tsunami was 4 m at Singkil and Simeulue Islands, and more than 1 m at Sibolga. In Nias

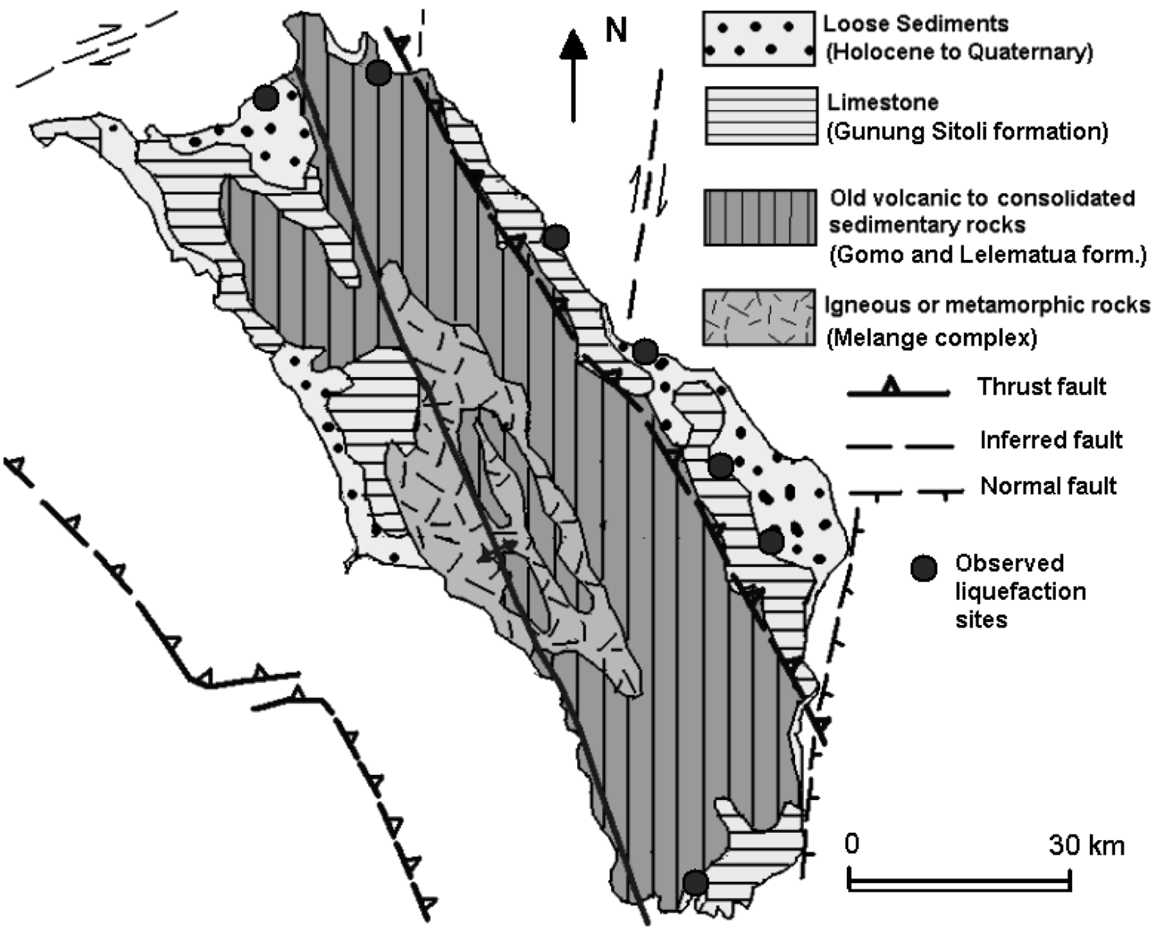

Figure 3. Geology of Nias Island (from Aydan et al., 2007 based on the map by Djamal et al., 1994).
Şekil 3. Nias adasının jeolojisi (Djamal vd. (1994)'nın haritasını esas alan Aydan vd. (2007)'den).

Table 1. Main characteristics of the earthquake.
Çizelge 1. Depremin başlıca özellikleri.

Institute	M	Mw	LAT (N)	LON (E)	DEP (km)	NP1 strike/dip/rake	NP2 strike/dip/rake
USGS	8.7	8.7	2.09	97.016	21.0	251/4/29	132/88/93
HARVARD	-	8.6	1.64	96.980	24.9	329/7/109	130/83/88

Table 2. Rupture and slip characteristics of the earthquake fault.
Çizelge 2. Deprem fayının kırılma ve atım özellikleri.

Parameters	Yagi (2005)	Yamanaka (2005)	Konca et al. (2006)	Borges et al. (2005)
Strike/Dip/rake	329/14/115	320/12/104	325/10/110	330/10/106
Moment tensor scale (Nm)	1.6 x10^{22}	1.3 x 10^{22}	1.0 x 10^{22}	0.82 x 10^{22}
Rupture duration time (s)	150 s	120 s	160 s	110
Rise time (s)			10-20	7.8
Rupture velocity (km/s)			2 km/s	3.3
Depth (km)	28	27	30	28
Rupture area (km^2)	150 x 470	120 x 250	400 x 60	400 x 125
Slip (m)	10 m	12	9	15

Island, the effects of the tsunami were observed by the JSCE team at Tuhemberua in the north and Sorake beach in the south, where wooden houses and two stories RC buildings collapsed or were heavily damaged (Aydan et al., 2005, 2007). According to the residents of these locations, the height of the tsunami was 4 to 5 m and 6 to 7 m, respectively. It was reported that the tsunami was up to 2 m high, and settlement of ground was observed in Banyak Islands. There were also reports of tsunami in other countries around the Indian Ocean, which were less than several tens of centimetres. The tsunami induced by this earthquake was much smaller than that of the 2004 event.

There was no acceleration record in any of Simeulue, Nias and Banyak Islands, or on the west coast of Sumatra Island. Therefore, it is almost impossible to know the exact ground motions induced by this earthquake. The only way is to infer the strong motions from the collapsed or heavily damaged structures such as reinforced concrete buildings, masonry or wooden houses and walls. The author inferred the MM intensity as IX from observations of the collapsed buildings. Furthermore, the maximum ground accelerations were estimated to range between 300 and 900 gals depending upon ground conditions, using the approach proposed by Aydan (2002) (Figure 5). Figure 5 also shows the inferred maximum ground accelerations and maximum ground velocities from the toppled simple structures observed in Gunung Sitoli and Teluk Dalam and their close vicinity using the earlier suggestions by Aydan (Aydan 2002, 2006; Aydan and Ohta, 2006). If the rise time and slip of an asperity are known, the maximum ground acceleration and velocity at the source area by the sliding on the asperity may be given in the following form, by assuming that the resulting acceleration can be represented by a sinusoidal function:

$$a_{\max} = 2\pi \frac{u_f}{\tau_r^2}; \quad v_{\max} = \frac{2u_f}{\tau_r} \qquad (1)$$

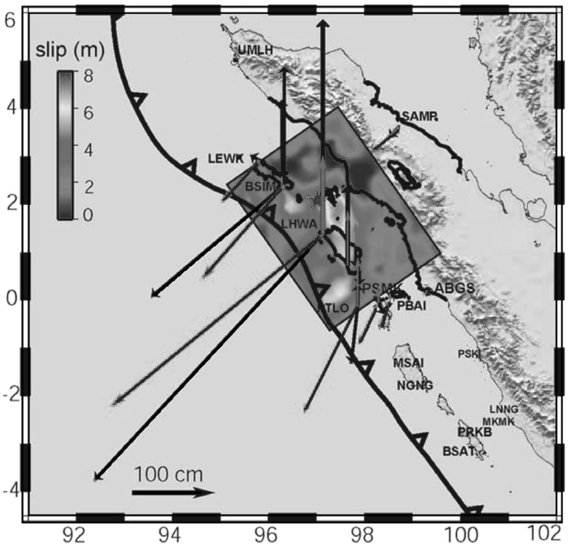

Figure 4. Comparison of estimated slip by Konca et al.(2006) with GPS observations.
Şekil 4. GPS gözlemleri ile Konca vd. (2006)'nın tahmin ettiği atımların karşılaştırılması.

If the estimated parameters used by Borges et al. (2005) are considered, the maximum ground acceleration and ground velocity at the source area are estimated to be 155 gal and 384 kine. On the other hand, if the estimations of Konca et al. (2006) are used, the estimated maximum ground acceleration and ground velocity at the source area would be 56 gal and 180 kine, respectively. Konca et al. (2006) stated that the maximum ground velocity could not be greater than 45 kine at the source area. However, the

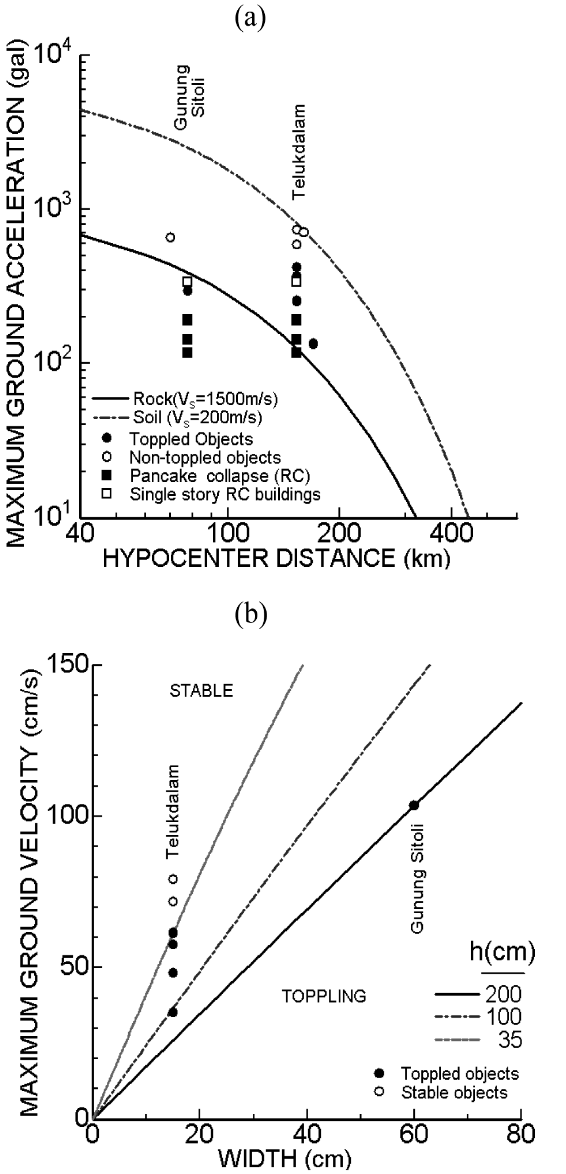

Figure 5. Comparison of estimated strong motion parameters with observations: (a) attenuation of a_{max}, (b) estimated maximum ground velocity.

Şekil 5. Gözlemlerle tahmin edilen kuvvetli yer hareket parametrelerinin karşılaştırılması: (a) a_{max}'ın azalımı ve (b) tahmin edilen en büyük yerhızı.

maximum ground velocity estimated from a toppled transformer is about 100 kine in Gunung Sitoli (78 km from hypocenter).

Aydan (2006, 2007) and Aydan and Ohta (2006) proposed some empirical relations to estimate the possible ground motions such as maximum ground acceleration and maximum ground velocity by taking into account the position of observation points with respect to fault orientations. This approach is adopted by assuming that the moment magnitude of the earthquake is 8.6 and the shear wave velocity of ground is 1000 m/s. This ground property will be equivalent to that of bedrock. However, it should be noted that these values would be generally amplified three to five times in soft ground. Figures 6 and 7 show the contours of maximum ground acceleration and velocity around the epicentral area of the earthquake. When the maximum ground accelerations are considered, the maximum value is 1500 gal at the epicentral area and gradually decreases with the distance from the hypocenter. The ground accelerations in Nias Island are expected to range between 380 gals to 1300 gals. The largest value is expected to be in the town of Lahewa. The ground acceleration will be greater than 650 gals in Gunung Sitoli and 380 gals in Teluk Dalam. Since there were many multi-story buildings with poor earthquake resistance in Gunung Sitoli and Teluk Dalam, it is no surprise that the ground motions were high enough to cause the collapse of such multi-story reinforced concrete structures, as also noted from Figure 5.

Similarly, the contours of the maximum ground velocity at the bedrock in Nias Island will range between 25 to 80 kines. Again these values can be amplified three to five times in soft ground, as observed in Gunung Sitoli, Teluk Dalam, Lahewa and Sirombu. Recent investigations by the author showed that bridge decks were displaced by 25 to 35 cm in Gunung Sitoli and Idano O'ou in spite of some restraints from their surroundings. The expected maximum ground velocities would be greater than 20 kines for these restrained structures.

Since the main purpose of this study is to estimate the ground motions near the Gunung Sitoli cave, it may be concluded from this discussion that the maximum ground acceleration is likely to be greater than 600 gal at the site.

Large seismic events beneath or in the vicinity of Nias Island are reported to had occurred. The events of 1843 (M7.2), 1861 (M8.5), 1907 (M7.6) and 2005 (M8.6) were just beneath the Island while the events of 1797 (M8.6), 1833 (M8.8), 1935 (M7.7) and 2004 (M9.3) took place to the north or south of Nias Island.

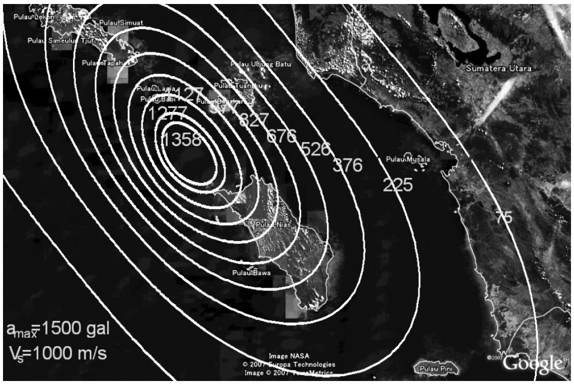

Figure 6. Maximum ground acceleration contours for the Nias Earthquake.
Şekil 6. Nias depremi için en büyük yer ivmesi eşdeğer eğrileri.

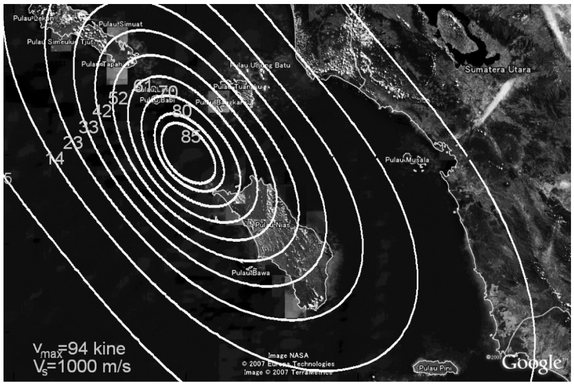

Figure 7. Maximum ground velocity contours for the Nias Earthquake.
Şekil 7. Nias depremi için en büyük yer hızı eşdeğer eğrileri.

THE GUNUNG SITOLI CAVE (TÖGİ-NDRAWA) AND ITS UNDERGROUND CLIMATE

The formation of Gunung Sitoli cave (Tögi-Ndrawa) is associated with the NE dipping thrust fault. Such faulting always induces various fractures within the fracture zone of the fault. These fractures are known to be R-R' (Riedel) fractures, T-fracture, S-fracture and P-fracture. Particularly R and T fractures would be caused by tensile stresses, and they are likely to create open spaces. If the seepage velocity of groundwater is high, these fractures are likely to be potential locations for the formation of karstic caves. The author investigated some karstic caves in Padang and Banda Aceh and this mechanism is confirmed by the site-investigations. One example is shown in Figure 8. The author feels that the same mechanism was the principal mechanism for the formation of the karstic Gunung Sitoli cave in Nias Island.

Figures 9 and 10 show the close up geology of the Gunung Sitoli cave and its location. The cave was formed in the Gunung Sitoli formation and several fold axes are recognised near the cave site. Figure 11 shows drawings of the plan and cross-sectional views of the cave. The cave is about 200 m long, 9-10 m wide and 8-12 m high with an overburden of 6-10 m. The entrance to the cave is one of the collapsed sections (CS1, CS2, CS3). Collapsed sections numbered CS2 and CS3 were observed and the collapse of the roof rock progressed to the ground surface forming sinkholes. Cross sections of the cave are shaped by the main fault dipping NE and secondary conjugate faults. An additional fault set, whose strike is perpendicular to the longitudinal cave axis, is also found and appears in the cave at regular intervals. The roof of the cave becomes higher at such locations and many stalactites and stalagmite growths occur near such faults.

Underground ventilation is natural and air flow takes place through the head difference between the entrance and the collapsed sections CS2 and CS3. The quality of air between CS1 and CS3, is generally good. Nevertheless, the air quality and air flow along the section between CS3 and the NW end of the cave gradually decreases. This part of the cave is damp and most of the cave inhabitants (bats) are found in this section. The air temperature and humidity range between 25-30 ^{o}C and 60-80% in the section between CS1 and CS3. However, the humidity increased to 90-95% near the NW end of the cave (L4) while the temperature change was quite small.

ROCK CLASSIFICATIONS AND STATIC STABILITY ASSESSMENTS

The rock surrounding the cave is limestone and its uniaxial compressive strength is expected to range between 20-40 MPa. The cave developed at a fault zone and at least 3 to 4 discontinuity sets exist in the rock mass. The bedding space is wide and is generally greater than 60 cm. The groundwater conditions can be considered damp to wet. Of course, there is no boring at the site. Nevertheless, the expected RQD values would range between 50-90%. Since the

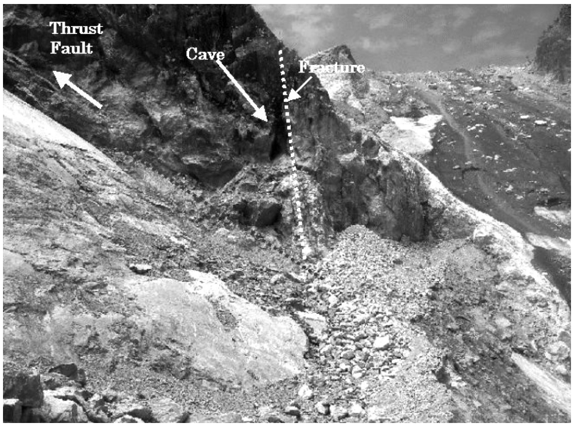

Figure 8. Formation by faulting of karstic caves in a limestone quarry near Padang.
Şekil 8. Padang yakınlarında faylanmaya bağlı olarak bir kireçtaşı ocağında karstik mağara oluşumu.

type of rock is limestone, the discontinuity surface with slickensides becomes either healed or rough. With these observations, the rock classification according to RMR classification (Bieniawski, 1974, 1989) may be estimated as given in Table 3.

If the Q-system (Barton et al., 1974) is used, the Q values obtained range between 6.25 and 15. If some interrelations between RMR and Q-values are used, the results would be quite similar to those computed above. There are two sections within the cave where roof collapse took place and migrated up to ground surface. At these two locations, the width of the cave ranges between 16 to 20 m. The stability of the cave can be analysed using empirical and analytical techniques. Barton et al. (1974) suggested an empirical line for the non-supported span of the underground openings as shown in Figure 12. Barton (1976) also suggested the following formula between the unsupported span (the unit is m) and the Q-value

Figure 9. Location map of Tögi Ndrawa cave in Nias Island.
Şekil 9. Nias adasında Tögi Ndrawa mağarasının yerbulduru haritası.

$$L = 66 \log Q + 2 \quad (2)$$

Lang (1994) drew two empirical bounding lines for the span between stable and unstable openings on the basis of observations in mines, as shown in Figure 12.

The critical limiting span of the underground opening based upon the arching theory can be given in the following form (i.e. Aydan, 1989; 1990; Aydan et al. 2007):

$$L = \sqrt{\frac{\sigma_{cm}}{\gamma} \xi H} \quad (3)$$

Table 3. Rating of rock mass according to RMR classification.
Çizelge 3. RMR sınıflamasına göre kaya kütlesi değerlendirilmesi.

Property	Description	Rating
Uniaxial compressive strength	20-40 MPa	2-4
RQD	50-90%	13-17
Discontinuity spacing	0.6 m or greater	15-20
Discontinuity condition	Unweathered, hard filling, rough, 0.1-1.0 mm aperture, persistence 10-20 m	20-25
Groundwater	Damp to wet	7-10
	Basic RMR	57-76

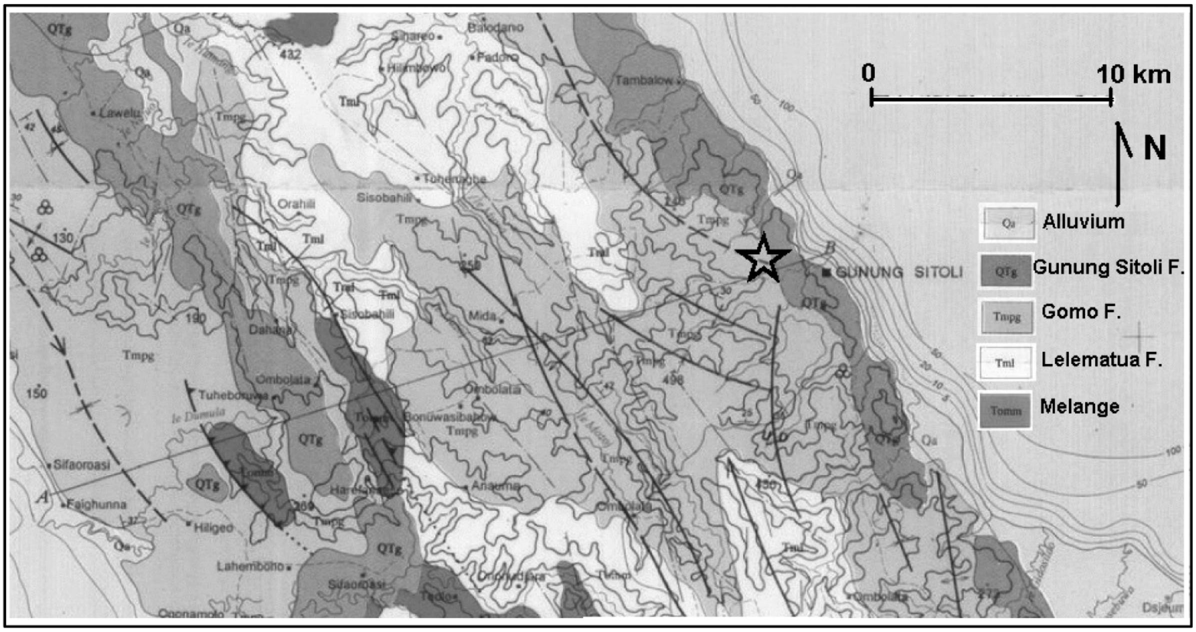

Figure 10. Geology in the close vicinity of the cave (modifield from the map by Djamal et al., 1994).
Şekil 10. Mağara yakınlarının jeolojisi (Djamal vd. (1994)'den değiştirilerek).

Where σ_{cm}, γ and H are uniaxial compressive strength and unit weight of rock mass and overburden height, respectively. The constant ξ is related to the stress distribution within the arch. If a triangular distribution for arching stress is assumed throughout the roof, it has a value of 4/3. However, if a certain length of vertical crack is assumed in the center of the roof and abutments, the value of constant ξ would be obtained from the minimization procedure as 3/2. The uniaxial compressive strength of rock mass can be obtained from the following empirical relation proposed by Aydan and Dalgıç (1998) and Aydan and Kawamoto (2000)

$$\sigma_{cm} = \frac{RMR}{RMR + \beta(100 - RMR)}\sigma_{ci} \quad (4)$$

Where β and σ_{ci} are empirical coefficient and uniaxial compressive strength of intact rock, respectively. Aydan and Dalgıç (1998) suggested that the value of β could be taken as 6 on the basis of experimental data from construction sites in Japan. The estimations of a limiting span by this arching theory approach are plotted in Figure 12 for an overburden height of 5 and 10 m by assuming the intact uniaxial strength of intact rock as 25 MPa on the basis of similar rock in Ryukyu Island (Aydan and Tokashiki, 2007). For the given conditions of Nias Cave, the empirical estimations given by the arching theo-

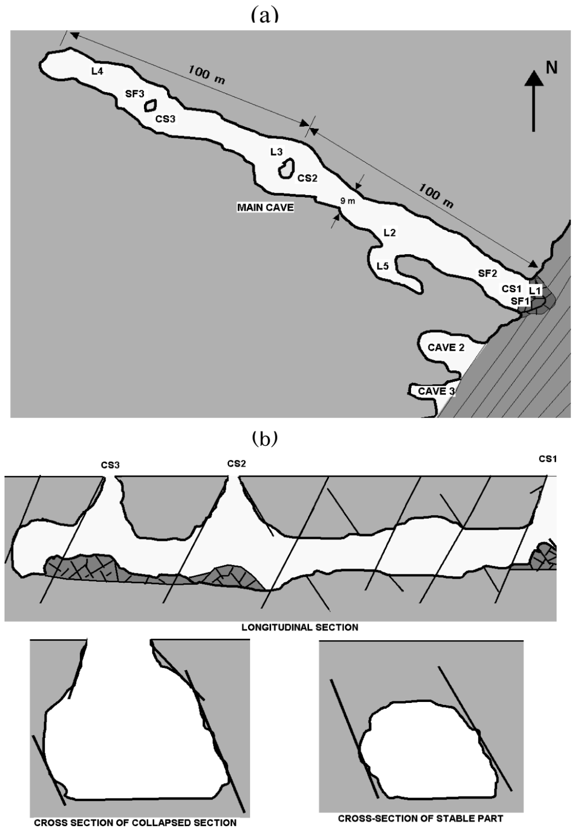

Figure 11. (a) Plan, and (b) longitudinal and cross sections of the Gunung Sitoli cave (not-to-scale).
Şekil 11. Gunung Sitoli mağarasının (a) planı ve (b) boyuna ve enine kesitleri (ölçeksiz).

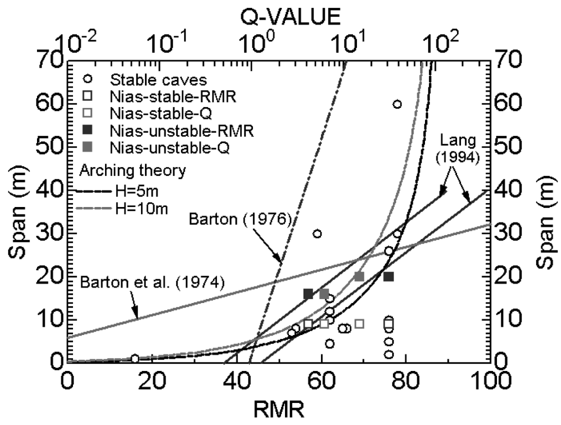

Figure 12. Comparison of Gunung Sitoli cave data with empirical criteria.

Şekil 12. Gunung Sitoli mağarası verilerinin görgül ölçütlerle karşılaştırılması.

ry and the lower bound line of Lang (1994) are in good agreement with observations while the estimations by the empirical relations proposed by Barton et al. (1974) and Barton (1976) are not compatible with observations.

SEISMIC DAMAGE AND ITS ASSOCIATIONS WITH THE 2005 GREAT NIAS EARTHQUAKE AND PREVIOUS EVENTS

Seismic damage to the Gunung Sitoli cave may be divided according to old and new seismic events and they can be categorized as follows:

a) Stalactite fall

b) Stalagmite fracturing and sometimes toppling

c) Vertical and horizontal off-setting of fractured stalactite and stalagmites.

d) Ductile bending of stalactite and stalagmites

e) Growth of stalagmites over fallen stalactites

The new events can be directly related to the 2005 Great Nias earthquake. The old events may be related to previous events and they may be identified through the height of stalagmites on the fallen stalactites. However, the growth rate of stalactites and stalagmites is necessary for dating such events. The data from Japanese caves in tropical zones and mainland indicates that the growth rate would range between 0.1 to 0.143 mm/year (Aydan and Tokashiki 2007).

Location 1: This is just the entrance to the cave and it faces SE outside. Three large stalactites were fallen down. The length and average diameter of the stalactites were 150 cm - 45 cm, 130 cm - 60 cm and 160 cm - 65 cm, respectively (Figure 13). In addition, there was a rockfall from the roof, which was about 4 m inside the entrance.

Location 2: At this location various forms of damage were observed (Figure 14). A column was ruptured with a separation of about 20-25 mm and 40 mm horizontal offset and the fractured part was healed. The same column was newly ruptured at 38 cm above the previous crack location. Two stalagmites with a height of 16-17 cm were found on the floor of the cave. Furthermore, a slab was separated by 40cm from the NE wall and there was a stalagmite growth with a height of 50 mm at the back of the separated block.

Location 3: A large roof collapse had occurred and the diameter of the cave is about 20 m at this location. On the NE wall of the cave, the surface of the NE dipping fault can be observed (Figure 15a) Although the solution of the surface of the fault made it difficult to observe the striations, it is possible to recognise a sense of the movement of the fault (Figure 15b).

Location 4: This location is very close to the NW end of the cave. This part of the cave has many fallen rockblocks and stalactites from the roof (Figure 16). The height of stalagmatites ranges between 5 to 16 cm. At this location, a column, which was broken by much earlier seismic events, was newly ruptured and was laterally displaced, as seen in Figure 17a. Another interesting observation was the re-rupturing of

Figure 13. Fallen stalactites and rock blocks near the entrance (Location 1).

Şekil 13. Mağara girişi yakınlarında düşmüş sarkıtlar ve bloklar (lokasyon 1).

Figure 14. Various forms of damage at Location 2.
Şekil 14. Lokasyon 2'de değişik hasar şekilleri.

previously ruptured sections. There was a new stalactite growth of about 25 mm in length and it was ruptured, probably 2005 by the Great Nias earthquake.

DISCUSSIONS AND CONCLUSIONS

Ground shaking and/or permanent ground movements may induce damage to speleothems during earthquakes. Depending upon the frequency characteristics of earthquake waves, some speleothems may be more prone to heavier shaking. Table 4 summarizes the natural frequency characteristics of speleothems (Aydan and Tokashiki, 2007). Depending upon the damping characteristics of speleothems, the amplification of ground acceleration would occur. For a velocity proportional damping of 10%, the amplification of ground acceleration would be limited to a range between 4 to 6.

Stalactites are much more slender than stalagmites. Furthermore, the axial stress acting on stalactites would be tensile, while it would be compressive for stalagmites under static conditions. However, it may be compressive when stalactites and stalagmites grow to constitute a single column. Speleothems can be considered to be cylindrical cantilever beams. If a seismic

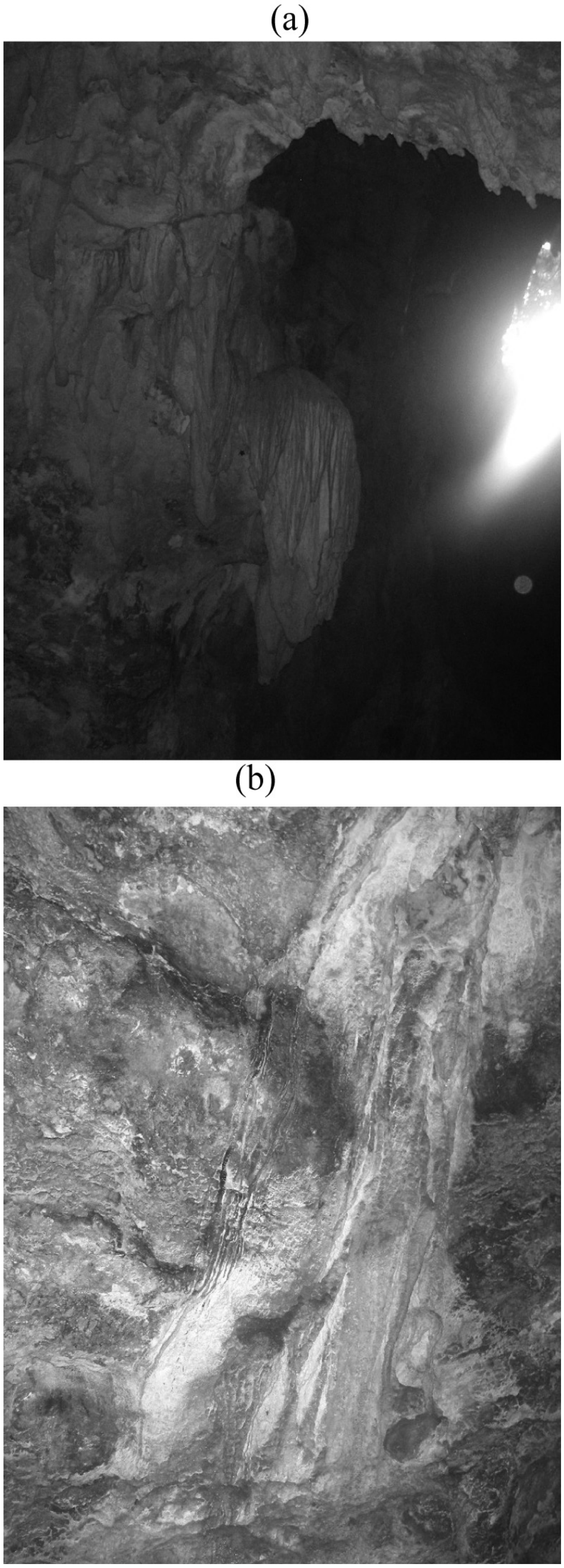

Figure 15. Views of the cave and fault at location 3 (CS3).
Şekil 15. Lokasyon 3'te (CS3) mağaranın ve fayın görünümleri.

Table 4. Natural frequency characteristics of speleothems (from Aydan and Tokashiki, 2007).
Çizelge 4. Sarkıt ve dikitlerin doğal salınım özellikleri (Aydan ve Tokashiki, (2007)'den).

Vibration mode	Natural frequency
Longitudinal	$f_n = n\frac{1}{2L}V_p$, n=1,2,3,
Transverse	$f_n = n\frac{1}{2L}V_s$, n=1,2,3
Cantilever beam	$f_1 = \frac{1.875^2}{2\pi}\sqrt{\frac{EI}{mL^4}}$, first mode
Built-in beam	$f_1 = \frac{\pi}{2}\sqrt{\frac{EI}{mL^4}}$, first mode

L: length; Vp: Longitudinal wave velocity; Vs: Transverse wave velocity; E: Elastic modulus; m: mass; I: inertia moment of area.

(a)

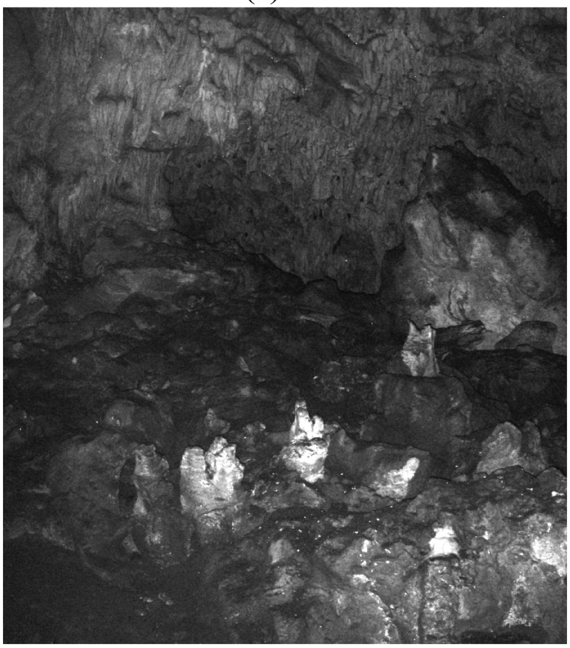

(b)

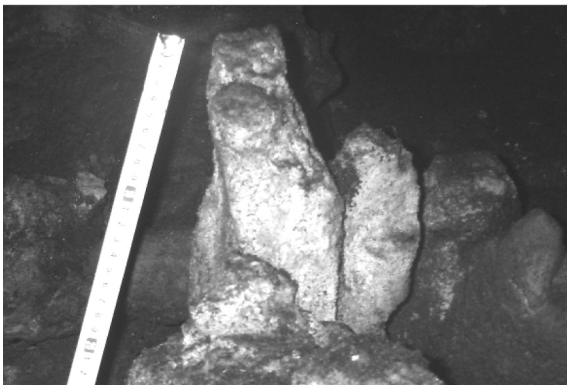

Figure 16. Stalagmite growths on fallen stalactites.
Şekil 16. Düşen sarkıtlar üzerinde dikitlerin büyümesi.

(a)

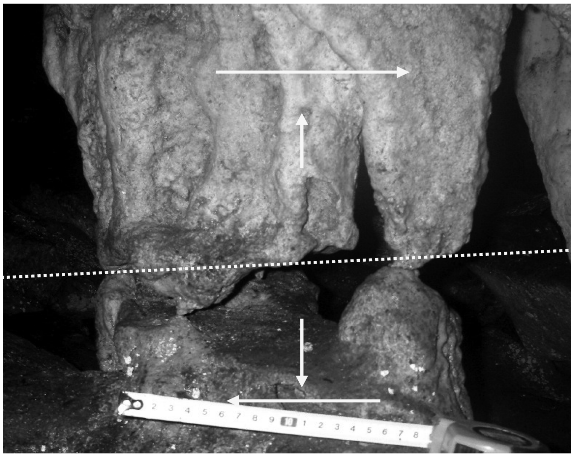

(b)

Figure 17. Re-rupturing of speleothems (Location 4): (a) re-rupturing of a speleothem, (b) re-rupturing of stalactite (the separation is about 25-30 mm).
Şekil 17. Sarkıt ve dikitlerin yeniden kırılması (Lokasyon 4): (a) birleşik sarkıt ve dikitin yeniden kırılması ve (b) sarkıtın yeniden kırılması (ayrılma yaklaşık 25-30 mm).

coefficient approach is adopted, the fiber stress at the base of a speleothem can be written in the following form (i.e. Aydan and Kawamoto, 1992)

$$\sigma_t = \pm\frac{W}{A} + \frac{\eta W\bar{h}}{I}\frac{t}{2} \quad (5)$$

where,

W: weight of speleothems,

A: base area of speleothems,

$\bar{h}$: distance of the center of gravity of speleothem from the base,

t: width or diameter of speleothem,

I: Second inertia moment of base area of speleothem,

η: seismic coefficient.

It should be noted that if a crack were initiated during shaking, it would end in the fall of stalactites (see discussion by Aydan and Kawamoto, 1992). Therefore, the crack initiation will directly correspond to the maximum ground acceleration acting on a stalactite. Figure 18 shows a simple computation for assessing the stability of speleothems by using the seismic coefficient approach.

If the earthquake does not affect the overall stability of caves, stalactites are more prone to be damaged by the earthquake when compared with stalagmites. Speleothems are generally made of calcite crystals and their tensile strength is generally greater than 2 MPa.

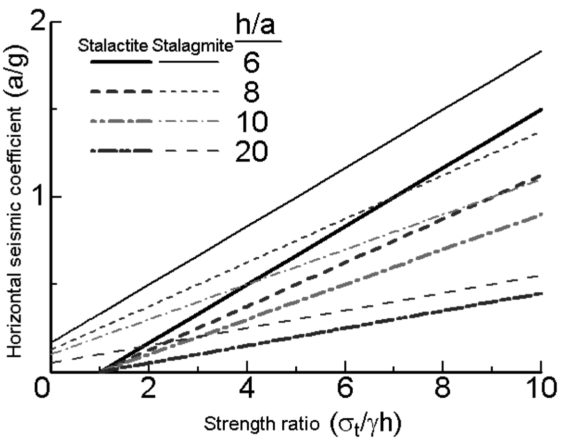

Figure 18. Estimated tensile strength of speleothems from the seismic coefficient method.
Şekil 18. Sarsıntı katsayısı yöntemi ile tahmin edilen sarkıt ve dikitlerin çekme dayanımı.

However, if they have impurities such as clayey material, their tensile strength may be drastically reduced. The unit weight of stalactites and stalagmatites generally ranges between 21-25 kN/m^3.

The expected ground motions in the vicinity of the Gunung Sitoli cave is more than 600 gals. The slenderness ratio (*h/a*) of the fallen stalactites ranges between 4.5 and 6. Therefore, the expected tensile (bonding) strength of the stalactites may range between 120-180 kPa (see Figure 18). Under static conditions, 5-8 m long stalactites may be sustained by such tensile strengths.

The healing of fractures with a separation of 20-25 mm at locations 2 and 4, implies a large previous seismic event. If the growth rate of 0.143mm/year is adopted, such an event could have been taken place 140 to 175 years before the present. This roughly corresponds to the 1861 event (M8.6) just beneath Nias Island or to the 1833 event (M8.8) to the south of Nias Island. The new fractures shown in Figures 14 and 17 are definitely associated with the 2005 Great Nias earthquake. Stalagmite growths on fallen stalactites at locations 2 and 4 indicate that there were very large seismic events 350-500 years and 1100-1600 years ago.

As pointed out by Forti (1998), Gilli (1999) and Gilli et al. (1999), the damage to spleothems in karstic caves may be induced by earthquakes and they may be used for dating unkown events in the seismological past of their regions. This study is a further contribution to such studies and provides a specific example from Nias Island, which experienced the M8.6 Great Nias earthquake. This study is probably the first of its kind in Indonesia to associate the damage to speleothems in the caves of Nias Island. The author expects that similar damage could exist in caves in other seismically active parts of Indonesia.

ACKNOWLEDGEMENTS

The author particularly thanks to Mr. F. Nakajima of CTI Engineering International, Tokyo, and Mr. T. Suzuki of the Indonesia Branch of Tobishima Company as well as local engineers of the Public Works Department in Nias Island for their help and guidance during the site investigation.

REFERENCES

Aydan, Ö., 1989. The stabilisation of rock engineering structures by rockbolts. PhD Thesis, Nagoya University, Japan.

Aydan, Ö., 1990. The effect of rockbolts on arching. Madencilik, 30(2), 33-40 (in Turkish).

Aydan, Ö., 2002. The inference of the earthquake fault and strong motions for Kutch earthquake of January 26, 2001. Proceedings of the Symposium on the Records and Lessons from the Recent Large Domestic and Overseas Earthquakes. Japan Earthquake Engineering Society, Tokyo, 135-140.

Aydan, Ö., 2006. Geological and seismological aspects of Kashmir earthquake of October 8, 2005 and a geotechnical evaluation of induced failures of natural and cut slopes. Journal of the School of Marine Science and Technology, Tokai University, 4(1), 25-44.

Aydan, Ö., 2007. Inference of seismic characteristics of possible earthquakes and liquefaction and landslide risks from active faults (in Turkish). The Proceedings of 6th National Conference on Earthquake Engineering of Turkey, Istanbul, Vol.1, 563-574.

Aydan, Ö., and Kawamoto, T., 1992. The stability of slopes and underground openings against flexural toppling and their stabilisation. Rock Mechanics and Rock Engineering, 25(3), 143-165.

Aydan, Ö., and Dalgıç, S., 1998. Prediction of deformation of 3-lanes Bolu tunnels through squeezing rocks of North Anatolian Fault Zone (NAFZ). Reg. Symp. On Sedimentary Rock Engineering, Taipei, 228-233.

Aydan, Ö., and Kawamoto, T., 2000. The assessment of mechanical properties of rock masses through RMR rock classification system. GeoEng2000, UW0926, Melbourne, Australia (on CD).

Aydan, Ö., and Ohta, Y., 2006. The characteristics of strong ground motions in the neighborhood of earthquake faults and their evaluation. A Symposium on the Records and Lessons from the recent large domestic and overseas earthquakes. Japan Earthquake Engineering Society, Tokyo, 114-120.

Aydan, Ö., and Tokashiki, N., 2007. Some damage observations in Ryukyu limestone caves of Ishigaki and Miyako Islands and their possible relations to 1771 Meiwa earthquake. Journal of the School of Marine Science and Technology, Tokai University, 6(1), 23-40.

Aydan, Ö., Miwa, S., Kodama, H., and Suzuki, T. 2005. The characteristics of M8.7 Nias earthquake of March 28, 2005 and induced tsunami and structural damages, Journal of the School of Marine Science and Technology, Tokai University, 3(2), 66-83.

Aydan, Ö., Miwa, S., Kodama, H., and Suzuki, T., 2007. Support activities of JSCE and EWoB-Japan for Nias Island following the Great Nias earthquake of 2005. The International Symposium on Disaster in Indonesia (ISDI): Problems & Solutions, Paper No: MS-3 (on CD).

Aydan, Ö., Tano, H., and Geniş, M., 2008. Assessment of long-term stability of an abandoned room and pillar underground lignite mine. Turkish Journal of Rock Mechanics, 16, 1-22 (in Turkish).

Barton, N., 1976. Unsupported underground openings. In Rock Mechanics Meeting, Swedish Rock Mechanics research Foundation, Stockholm, 61-94.

Barton, N., Lien, R., and Lunde, I., 1974. Engineering classification of rock masses for the design of tunnel supports. Rock Mechanics, 6(4), 189-239.

Bieniawski, Z.T., 1974. Geomechanics classification of rock masses and its application in tunnelling. Proceddings of the Third International Congress on Rock Mechanics, ISRM, Denver, IIA, 27-32.

Bieniawski, Z.T., 1989. Engineering Rock Mass Classifications. John Wiley and Sons, New York.

Borges, J. F., Caldeira, B., and Bezzeghoud, M., 2005. Source Rupture Process of the Sumatra, Indonesia Earthquake (M_w=8.6) of 28 March 2005. Preliminary results. http://www.cge.uevora.pt/, April, 2005.

Djamal, B., Gunawan, W., Simandjuntak, T.O., and Ratman, N., 1994. Geological map of Nias Sheet, Sumatera. Geological Research and Development Center.

Forti, P., 1998. Seismotectonic and paleoseismic studies from speleothems: The state of the art: Han 98-Tectonique: Karst et Seismes, 79–81.

Gilli, E., 1999. Evidence of paleoseismicity in a flowstone of the Observatoire cave (Monaco). Geodinamica Acta, 12, 159–168.

Gilli, E., Levret, A., Sollogoub, P., and Delange, P., 1999. Research on the February 18, 1996, earthquake in the caves of the Saint-Paul-de-Fenouillet area (eastern Pyrenees, France. Geodinamica Acta, 12, 143–158.

HARVARD, 2005. Harvard Centroid Moment Tensor, Department of Earth and Planetary Sciences, Harvard University, Cambridge, MA, USA.

Konca, A.O., Hjorleifsdottir, V., Song, T. A., Avouac, J.P., Helmberger, D.V., Chen Ji, Sieh K., Briggs, R., and Meltzner, A., 2006. Rupture Kinematics of the 2005 *M*w 8.6 Nias–Simeulue Earthquake from the Joint Inversion of Seismic and Geodetic Data. Bulletin of the Seismological Society of America, 97(1A), S307–S322,

Lang, B., 1994. Span design for entry type excavations. M.Sc. Thesis, British Columbia University, Vancouver, BC.

OCHA (United Nations Office for the Coordination of Humanitarian Affairs), 2005. Earthquake OCHA Situation Report No.2, Indonesia Earthquake, 28 March, 2005., http://www.reliefweb.int/rw/dbc.nsf/, April, 2005.

Tokashiki, N., and Aydan, Ö., 2003. Characteristics of Ryukyu Limestone and its utilization as a building stone in historical and modern structures. International Symposium on Industrial Minerals and Building Stones, Istanbul, 311-318.

USGS, 2005. U.S. Geological Survey, National Earthquake Information Center, Golden, CO, USA. Magnitude 8.7 Northern Sumatra, Indonesia, 2005 March 28 16:09:36 UTC. http://earthquake.usgs.gov/, USA, April, 2005.

Yagi, Y., 2005. Magnitude 8.7 Northern Sumatra Earthquake. Building Research Institute. http://iisee.kenken.go.jp/staff/yagi/eq/Sumatra2005/.

Yamanaka, K., 2005. Earthquake in Indonesia, March 28, 2005 (Magnitude 8.7), EIC Seismology Note, No.164. Earthquake Research Institute, University of Tokyo (in Japanese), April, 2005.